MODELING SOIL CARBON SPATIAL VARIATION: CASE STUDY IN THE PALOUSE REGION

Armen R. Kemanian

Department of Crop and Soil Sciences, The Pennsylvania State University University Park, PA

David. R. Huggins, David P. Uberuaga

USDA-ARS Land Management and Water Conservation Research Unit Pullman, WA

ABSTRACT

Soil organic carbon (C_s) levels in the soil profile reflect the transient state or equilibrium conditions determined by organic carbon inputs and outputs. In areas with strong topography, erosion, transport and deposition control de soil carbon balance and determine strong within-field differences in soil carbon. Carbon gains or losses are therefore difficult to predict for the average field. Total C_s ranged from 54 to 272 Mg C ha^{-1}, with 42% (range 25 to 78%) of C_s in the top 0.3-m of the soil profile. Globally, the C_s in the topsoil (0.3-m) and subsoil (0.3 – 1.5-m) at the CAF shows overall an expected pattern of soil erosion of convex and upland landscape locations, and accumulation of C_s in concave and lowland locations. Locally, however, describing a point as upland or lowland landscape position provides limited information to predict total C_s or its distribution with depth. The topsoil C_s content is coupled with the local aboveground productivity, indicating that carbon inputs play a role at maintaining the current C_s across the landscape. No such relationship was found for subsoil C_s. Based on simulations of soil carbon accretion and cycling, much of the topsoil C_s can be at equilibrium with inputs, but the subsoil could be losing carbon at a slow but steady rate for much of the farm.

Keywords: soil carbon, spatial variation, modeling

INTRODUCTION

Designing management strategies that can reduce emissions or increase the storage of soil organic carbon (C_s) in farmland are critical for agriculture to contribute to the mitigation of greenhouse gas emissions. The dryland cropping Palouse region of eastern Washington has spatially variable soil and topographic conditions that determine a complex temporal pattern of microclimate, water

storage and movement, erosion, and nitrogen dynamics (Busacca and Montgomery, 1992) that reflect in large spatial variation of C_s. This variation reflects the C balance (inputs minus outputs) spatial variation in the landscape.

Site-specific carbon inputs consist of residues and roots and deposition of residues and C_s from eroded areas. Losses are controlled by microbial (and micro-faunal) respiration that use residues and soil organic matter as substrate, and by soil erosion losses. Once erosion is controlled or minimized, the carbon balance of a single layer is determined by the input rate (C_i, Mg C ha^{-1} yr^{-1}), the humification rate (h, yr^{-1}), and by the soil apparent decomposition rate (k, yr^{-1}) as follows:

$$dC_s/dt = hC_i - kC_s. \quad [1]$$

This equation was first proposed by Hénin and Dupuis (1945) and while mathematically simple, is adequate for hypothesis development and testing, and for field-level data interpretation (Huggins et al., 1998a,b). Mixing among layers is not considered in this equation but can be easily added in a numerical implementation.

The application of this equation in a distributed manner across the landscape is not without challenges for (1) all component of C_i are spatially variable and difficult to predict (aboveground and root production) or poorly understood (rhizodeposition), (2) it requires knowing C_s distribution, (3) it requires knowing accurately h and k, and (4) soil properties needed to simulate soil processes have marked spatial variation (e.g. Pachepsky et al., 2001). Despite these difficulties, Clay et al. (2005) strongly suggested that in corn-soybean rotation in east south central South Dakota, the residue input rate to maintain C_s levels varies with elevation, being larger in low elevation or depositional areas.

Our proposition is that different sections of the landscape can be sources or sinks of carbon and that managing the C_s balance is therefore a prime target for the application of precision conservation. Our objectives in this research were to investigate the C_s spatial distribution in the Cook Agronomy Farm of Washington State University, and to estimate the C balance as determined by inputs and decomposition rates across the landscape using the model C-Farm (Kemanian and Stockle, 2010). The model C-Farm has algorithms to compute the terms of Eq. [1] C_i, h, and k at daily time step in different soils layers.

MATERIAL AND METHODS

Soil carbon data from an intensively monitored farm in eastern Washington were analyzed to try to understand the main controls of the current levels of C_s in this typical field-section of the Palouse. The analysis was performed as to generate contrasting groups of observation regarding C_s content and distribution with depth. Within each group, simulations with the model C-Farm of continuous cereal cropping were executed to estimate the carbon inputs, inputs distribution with depth, turnover rates, and the overall C_s balance across the landscape.

The research site was the Cook Agronomy Farm (46° 47' N, 117° 5' W, 773-815 m elevation range) is located five km NE of Pullman, WA. The farm average slope is 11%, with maximum slopes of 33% with a topography representative of

the rolling hills of the Palouse region, albeit with a dominant west-facing aspect. Precipitation averages 520 mm per annum; summers are dry. Soils are silt loams developed in loessial deposits with intricately associated Palouse (Fine-silty, mixed, superactive, mesic Pachic Ultic Haploxerolls), Naff (Fine-silty, mixed, superactive, mesic Typic Argixerolls), Thatuna (Fine-silty, mixed, superactive, mesic Oxyaquic Argixerolls), Latah (Fine, mixed, superactive, mesic Xeric Argialbolls), and Staley (Fine-silty, mixed, superactive, mesic Calcic Haploxerolls) soils. The differences among soils reflect the hydrological regime (upland, dry: Staley; alluvial lowland: Latah) and presence (Naff, Thatuna) or absence of an argillic horizon.

A nonaligned, randomized grid sampling design with 369 geo-referenced points was overlaid in the southern 37-ha portion of the farm. Soil profiles were taken in 177 point within the grid and used to estimate soil carbon in the top 0.3 m and in the rest of profile (up to 1.5 m). Each sample was described and assigned a soil type. In addition depth of the A and argillic horizon (when present) were recorded. Grain yield from most of the 369 geo-referenced points and for multiple crops growing in six different rotations have been collected annually since 1999. Topographic data were derived from a 10x10-m grid DEM. Slope was calculated as the rate of change in elevation in the direction of the steepest descent. Aspect was converted from degrees rotating clockwise with the N as 0°, to a new scale (1 - cos[aspect - 30°])/2. The new scale ranges from 0 at aspect = 30° (N-NE aspect) to 1 at aspect = 210° (S-SW aspect) and is representative of the change in irradiance due to aspect. Plan curvature was calculated as the rate of change in aspect along a contour (radians m^{-1}) with convex (concave) topography having positive (negative) values (Gallant and Wilson, 2000). Profile curvature is the rate of change in slope down a flow line (Gallant and Wilson, 2000), with concave (convex) topography having positive (negative) values. The wetness index was calculated as the ratio between the slope and the corresponding upslope contributing area for a given point. Gentle slopes and greater upslope contributing areas give the minimum wetness index and indicate areas prone to water accumulation; conversely, high values indicate divergent convex ridges. Annual, clear sky irradiance was estimated based on latitude, slope, aspect, and shading from surrounding terrain and scaled to a maximum of 1.

The variables best explaining C_s variation were analyzed using Random Forests or RF (Breiman, 2001) and the data set classified using classification and regression trees or CART (Breiman et al., 1984). CART is a divisive classification method that uses binary partitioning to create increasingly homogeneous clusters of observations based on the association of the response variable and descriptor variables. The binary division generates branches with terminal nodes containing groups of observations. The method is extremely flexibly as it is not affected by co-linearity, has no-requirement of normality in data distribution, and digests categorical and continuous data. Random Forests is a variation of CART that, instead of using all information to build a single tree, uses about 2/3 of the data to build many trees (a forest) and the remaining 1/3 or out-of-bag sample to compute classification errors. At each node a sample of predictors is used to generate a split; CART uses all predictors at each node. For regression, each tree predicts an average expected value for each out-of-bag

observation. The average of all predictions is the RF regression estimate and is used to calculate the prediction error and the fraction of the variance explained by the model. The model has only two parameters, the number of trees to be constructed, and the number of predictors to be sampled at each node which is about 1/3 of the total number of predictors for regression (Liaw and Wiener, 2002), but the optimum number varies with the data set and number under analysis. A measure of the importance of each predictor variable is obtained by calculating how the prediction error increases when out-of-bag data for a given variable is permutated while all others are left unchanged, making RF extremely useful as an exploratory tool. To our knowledge, Random Forest has been seldom used, if ever, to analyze complex agricultural datasets comprising multiple variables with widely different statistical properties and exhibiting colinearity. When used in ecological studies it proved to be better or as good as any other multivariate method (e.g. Prasad et al., 2006; Rehfeldt et al., 2006).

The model C-Farm is a daily-time step cropping systems model that allows calculating the C_s balance using a one-pool C_s. The model has been described in detail in Kemanian and Stockle (2010). In C-Farm the C_s turnover rate and C_i humification rate depend non-linearly on C_s; the turnover rate is also affected by environmental and management controls. The environmental controls are soil moisture, temperature and air filled porosity. All components of the water balance are computed at a daily time-step except infiltration and redistribution of water within the soil profile which use a variable and sub-daily time step. Soil temperature is calculated for each layer using a simplified energy balance. Tillage mixes all state variables in the affected layers and increases the C_s turnover rate k but does not alter the humification rate h. The crop module of C-Farm is a simplification with a few variations of that of CropSyst (Stockle and Nelson, 2003). Organic N cycling is closely linked with that of C and the C/N ratio of the decomposing pool (residues, roots, root exudates and manure) as well as the availability of mineral nitrogen control the pool decomposition rate and resulting C/N ratio. C-Farm proved to be particularly suited to simulate C_s evolution in the long-term experiment, winter wheat – summer fallow sequence, at Pendleton, Oregon (Kemanian and Stockle, 2010).

RESULTS AND DISCUSSION

Regression and classification

For the 177 observations, the average (standard deviation) C_s for the profile, top 0.3-m and the subsoil was 131 (36), 56 (10), and 75 (30) Mg C ha^{-1}. At Pendleton, Oregon, the winter-wheat summer fallow plots have topsoil C_s levels of approximately 40 Mg C ha^{-1} (Rasmussen and Albretch, 1998; Kemanian and Stockle, 2010) while the average in the CAF is 57 Mg C ha^{-1}, 40% larger, due, in part, to the negative impact of summer fallow on soil C_s.

The relatively larger variation in subsoil C_s (Figure 1) reflects the differences in soil depth across the landscape, with lower C_s in eroded knobs and large accumulations in a few depositional locations (Figure 2). Parallel to the eastern and northern boundaries of this section of the farm runs a seasonal creek that

drains the larger watershed. The flat terrain bordering the creek is a floodplain that shows intermittently large accumulations of sub-soil C_s (Figure 2). The irregular accumulation of C_s suggests that erosion and deposition, and perhaps past transport to soil by tillage, determine a non-uniform accumulation of C_s.

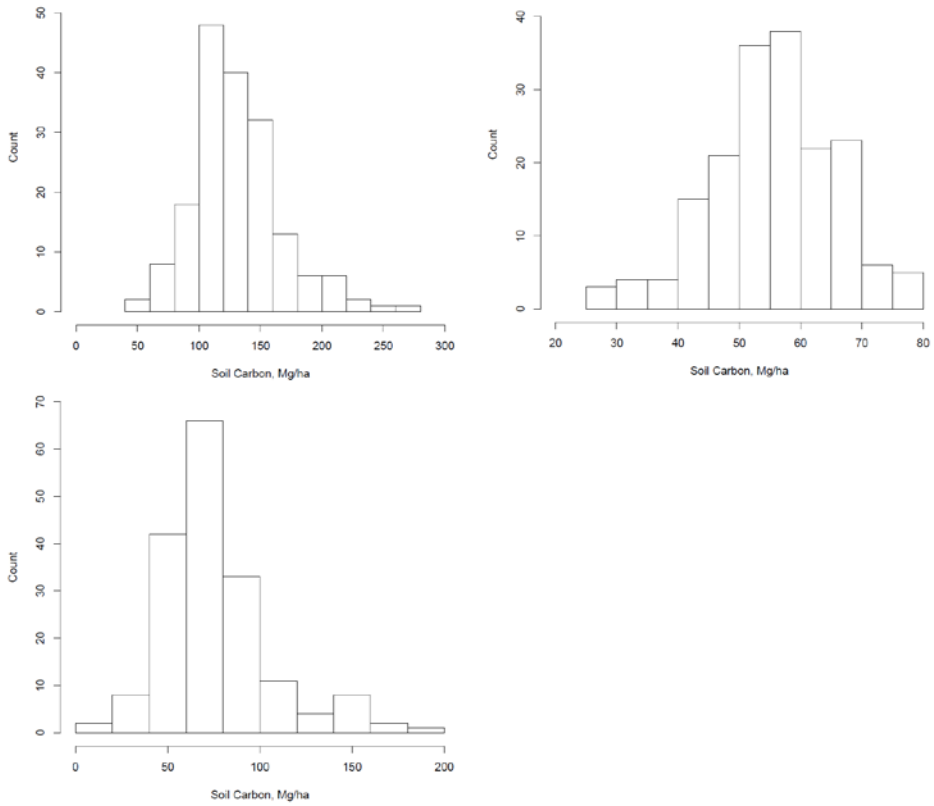

Figure 1. Frequency distribution of soil organic carbon in the profile (top panel), the top 0.3-m of the profile (middle panel) and between 0.3 and 1.5 m in Cook Agronomy Farm in eastern Washington. The total number of observation is 177.

While C_s shows spatial clustering (Fig. 2) the overall pattern of C_s distribution is not easy to predict except for a few cases. North-facing steep slopes can have high or medium C_s accumulation in the top soil depending on which north-slope and which specific location in the north-slope is selected. Equally steep southern or east facing slope are obviously eroded.

Regression analysis with RF that includes average relative yield of a location, a biological indicator of productivity, topographic, and soil attributes was able to explain, at best, 37% and 43% of the observed variation in C_s in the top soil and subsoil, respectively. While this is a preliminary analysis, a few noteworthy features are highlighted. In the topsoil, site productivity or carbon inputs are related to C_s levels, while in the subsoil other variables are more relevant. This indicates control of C_s in soil by current or short-term inputs and historic factors explaining subsoil C_s. The inclusion of variables such as depth of the A horizon or depth to the Bt horizon can give relatively obvious results, as thicker A horizons or deeper Bt horizons will usually be associated with high C_s content in

agricultural soils. When depth to A horizon is removed, depth to Bt horizon increases in importance at explaining the variation as shown for the subsoil. The soil EMC measurements in spring seem to provide a valuable integrated measure of soil properties. Somewhat surprisingly, presence or absence of the Bt horizon, prevalent in about ½ of the farm, was weakly related to C_s. It is interesting that when the variable site productivity is removed, topographic attributes such plan and tangential curvatures, which discriminate between convex, divergent portions of the landscape, and concave positions, become important at explaining the observed variation. Further analysis should explore a systematic removal / inclusion of topographic and soil attributes from freely accessible soil databases, soil attributes obtained from soil sampling, and yield monitoring data.

To facilitate the selection of simulation points, we ran CART on the topsoil and the subsoil. Ideally, variables that have local importance but have no relation with actual processes such as easting and northing (the point coordinates) should not be included in this analysis, but we did so to generate groups as homogeneous as possible for the simulation. Running the analysis for the topsoil and the subsoil separately will not generate the same classes.

For the topsoil, depth of A horizon, plan curvature, flow accumulation, EMC and depth of the Bw horizon were the main drivers to shape the tree (Fig. 3). Relatively thin A horizons (< 0.6 m) in convex positions with shallow Bw horizon have the lowest average C_s (43 Mg C ha^{-1}), while deep A horizons in depositional areas have the highest C_s (64 Mg C ha^{-1}). Summary information for each group is presented in Table 2. Removing the A horizon places the site productivity as the first split. Interestingly, for the subsoil the plan curvature, irradiance (a measure of aspect and slope) and slope controlled the tree growth (Fig. 4). The points with lowest subsoil C_s were at convex or south facing (high irradiance) and high slope locations (average C_s of 47 Mg C ha^{-1}), and conversely, the points with highest C_s were at depositional convex areas or in areas with moderate curvature with lower irradiance load. This can be an indirect indication of the effect of the prevailing SW winds that cause snow drift and accelerated drying of south facing slopes. These observations are in broad agreement with what can be gleaned from Fig. 2 and Table 1. Both RF and CART provide strong evidence that a relationship exists between the response variable with a given predictor, but unraveling the mechanisms behind the relationship requires interpretations that are not straightforward.

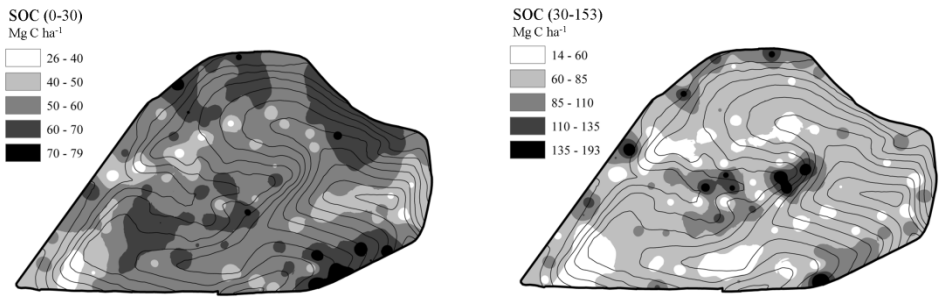

Figure 2. Soil carbon in the topsoil (0.3-m) of the soil profile (top panel), and in the subsurface (0.5 and 1.5 m) of the soil profile (bottom panel) in the Cook Agronomy Farm.

Table 1. Results of the regression with Radom Forests where soil organic carbon is the response variable and the list to the left of the table are predictor variable (crop, soil, and topographic attributes). The table shows the importance of each variable, and the bottom of the table the variation in C_s explained by the regression forest.

Predictor[1]	Topsoil organic carbon			Subsoil organic carbon			
easting	**9.61**	6.99		4.47	3.07		5.02
northing	3.33	7.12		4.15	3.46		5.38
soil	2.07	1.55	0.79	4.49	6.26	6.45	5.73
soil.sur	3.10	3.49	3.16	6.27	4.96	4.72	7.17
sub.horizon	3.55	1.52	1.29	4.89	5.06	6.62	4.81
site.productivity	**18.75**			5.29			6.67
Bt.ik	2.51	1.52	2.04	4.68	5.27	3.31	4.69
Bt	0.27	1.04	-0.51	2.07	2.54	2.98	4.06
Bk	1.63	-0.53	1.27	4.32	4.59	1.37	4.97
E	2.19	3.76	2.06	3.04	1.51	2.53	3.54
Bw	0.53	0.82	-0.97	1.80	1.82	1.39	2.76
A.depth	**13.18**	**15.65**	**14.55**	**16.99**	**17.76**	**18.44**	
Bt.depth	3.37	4.40	1.96	**9.19**	**10.47**	**10.26**	**12.99**
Bw.depth	6.16	7.97	7.87	5.50	4.23	3.46	6.53
irradiance	**7.91**	**11.59**	**10.26**	3.80	3.66	4.19	3.31
slope	5.32	5.53	5.64	2.12	0.46	1.09	1.90
aspect	6.35	6.19	3.94	5.02	3.22	2.56	3.81
curv.tan	5.82	8.08	6.73	**7.30**	**8.09**	**7.29**	**7.88**
curv.pln	7.73	**9.69**	7.72	7.10	6.99	6.43	**7.89**
cur.pro	3.49	5.04	1.88	**19.32**	**19.34**	**19.35**	**21.23**
flod	6.94	**9.37**	8.46	5.60	2.24	3.51	3.00
floa	2.97	1.26	2.19	-1.41	-0.29	-1.80	0.86
wet.index	4.83	6.61	5.74	0.03	1.51	-0.57	2.28
elevation	6.40	4.54	2.90	4.63	5.56	4.67	5.07
EMC spring 2000	**10.05**	**10.49**	**11.75**	**8.36**	**7.61**	**8.55**	**9.97**
EMC fall 2000	6.07	7.79	9.88	4.09	5.35	6.22	4.65
RMSE, Mg C ha^{-1}	8.1	8.5	8.4	22.4	22.5	22.5	23.3
Var explained, %	37.1	30.9	31.3	43.5	43.1	43.1	39.0

[1] easting and northing = coordinates of the points; soil = soil classification, soil.sur = SURGO soil classification; sub.horizon = subsoil horizon below A horizon (Bt, Bw, Bk, E); site.productivy = relative yield of the point as an average of 6 years of hand-samples; Bt.ik is the interpolated probability of finding an argilic horizon at the location; Bt, Bk, E, and Bw describe B horizons; A, B, and Bw.depth are the thickness (A) or top of the horizon (B); irradiance = relative irradiance of the site which depends on topography; slope, aspect, planar, tangential and profile curvature, and flow accumulation and wetness index are explained in Materials and Methods; EMC = electromagnetic conductivity measured in spring or fall of 2000.

The points for the simulation were selected based on the classes obtained with classification of the C_s topsoil (Fig. 3, Table 2). In this preliminary analysis we decided to use a rather astringent criterion to stop the tree growth using a high threshold in the MSE reduction required for a split to be valid and we obtained only 6 groups (Fig. 3) that are large and contain variation. Further refinement of the analysis will allow splitting into more homogenous groups.

Soil carbon dynamics simulation

Some characteristics of the simulation points are shown in Table 3. Points for groups 1, 2, and 3 are in south facing slopes, mostly convex, upslope positions with south facing slope. Point in group 5 is a concave south facing slope (Palouse

/ Naff). The points in groups 4 and 6 are in north facing slopes, and the Thatuna soil (group 6) in particular is a depositional area. Only simulations for the three most contrasting points are shown: groups 2, 4, and 6, with low, medium, and high total C_s. Point 6 has as much subsoil C_s as point 2 in the entire profile.

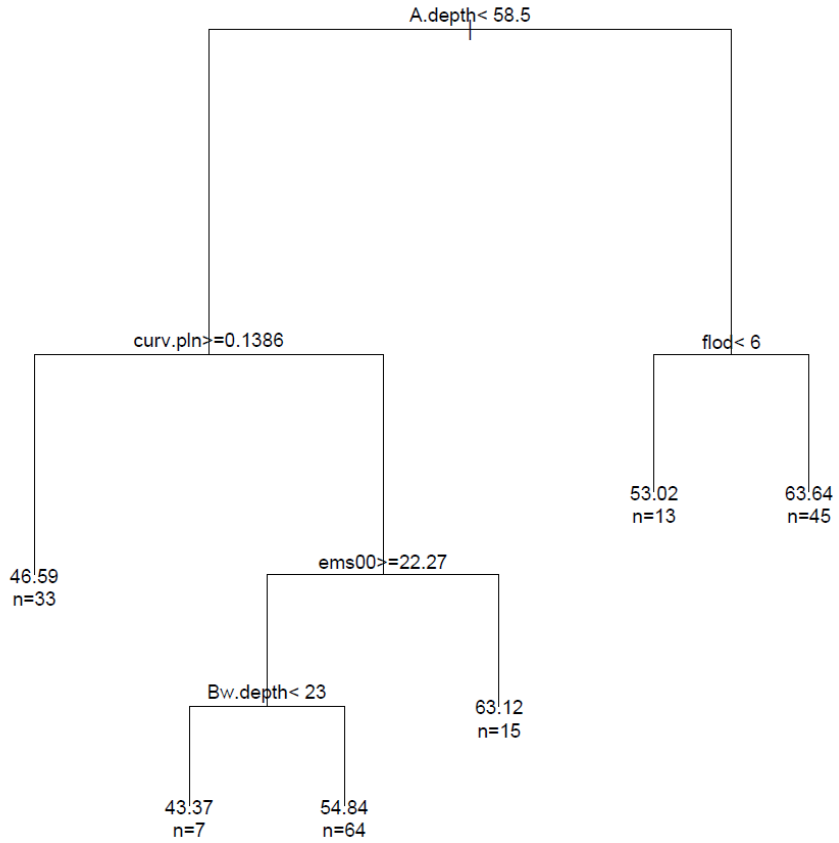

Figure 3. CART for soil organic carbon in the topsoil (A.depth = thickness of the A horizon, curv.pln = plan curvature, ems00 = electromagnetic conductivity in spring of 2000, Bw.depth = depth of the Bw horizon, flod = flow direction).

In this environment water availability is the main driver of productivity. The simulated water balance for the three points was similar (Table 4). Soil evaporation and runoff may have been underestimated. Return flow down the slope, particular where Bt horizons are present, was not simulated. On flat, homogeneous terrains this water balance is likely correct, because these soils have large water storage capacity (2.5 m of soil could store the average annual rainfall without drainage). The effect of wind direction in the water balance at each location was not included and can have a large local effect for (1) snow redistribution from south to north-slopes is obvious in the winter time; that produces drier south slopes and wetter north slopes, and (2) the effect of the prevailing SW winds on soil evaporation and crop transpiration in south slopes is not represented, and conversely, the lesser water demand in north slopes is not represented. If these factors were included, evaporation would increase in south slopes compared with that simulated, and runoff and drainage increase in the north slopes as is usually observed in the field in early spring. Despite these limitations, the simulations of the carbon balance are insightful.

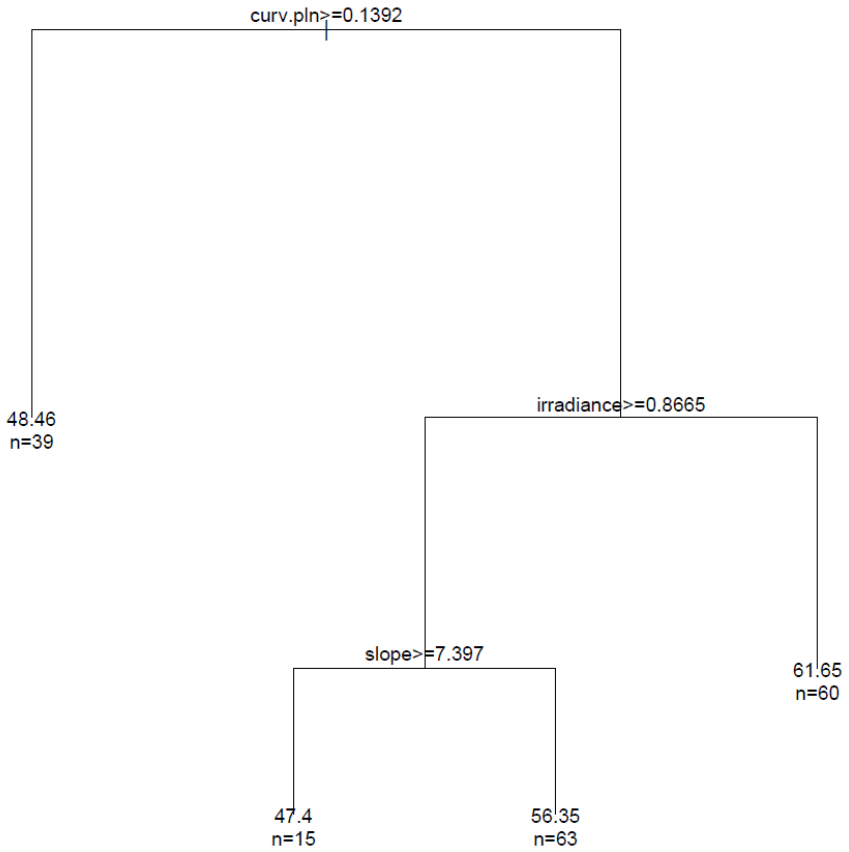

Figure 4. CART for soil organic carbon in the subsoil (curv.pln = plan curvature).

The topsoil at the different locations is near equilibrium conditions. A regression of the annual C_s balance against the initial C_s in that layer indicates that with inputs of 3 Mg C ha^{-1} yr^{-1} the topsoil C_s equilibrium content is 60 Mg C ha^{-1}. It also indicates that it is difficult to sustain that C_s level with less C inputs and that residue removal may lead to C losses unless replenished with other C inputs. Locations with topsoil C_s < 60 Mg C ha are prime targets for C storage if productivity and C inputs are increased. This is in agreement with the relationship found between top soil C_s and site productivity in the RF analysis.

Table 2. Summary characteristics of the grouping of observations based on CART as shown in Figure 3 (topsoil = 0.3 m, subsoil = 0.3 – 1.5 m, C_s = soil organic carbon). The C_s levels where qualitatively characterized as Low, Medium and High (L, M, H). The order of soil listing indicates which soil series is prevalent in the group.

Group (n)	C_s level	Topsoil C_s	Subsoil C_s	Profile C_s	A depth	Soil series
		---------- Mg ha^{-1} ----------			m	
1 (33)	ML	47	53	100	0.36	Naff/Palouse/Staley
2 (7)	L	43	52	95	0.19	Palouse/Naff
3 (64)	M	55	71	126	0.40	Palouse/Thatuna/Naff
4 (15)	MH	63	81	144	0.35	Palouse
5 (13)	M	53	74	127	0.67	Palouse/Naff
6 (45)	H	64	100	164	0.73	Thatuna/Palouse

Table 3. Characteristics of the points selected for the simulations. The soil organic carbon (C_s) as in Table 2. Site productivity (SP) averaged 0.63 for the entire farm, with minimum and maximum of 0.39 and 0.80, respectively.

Group	Soil series	SP	A depth	Slope	Landform	Topsoil C_s	Subsoil C_s	Profile C_s
				%		---------- Mg ha^{-1} ----------		
1	Palouse	0.65	0.46	1.3	Convex	46	56	102
2	Palouse	0.67	0.15	1.9	Convex	47	53	100
3	Palouse	0.63	0.44	3.9	Flat	54	72	126
4	Palouse	0.73	0.36	7.6	Convex	62	74	137
5	Palouse	0.58	0.62	4.7	Concave	53	76	128
6	Thatuna	0.59	0.66	5.4	Concave	64	125	189

Despite the attention that the topsoil has received regarding C cycling and storage, the largest impact on the long-term C_s balance can be in managing the subsoil. The simulation results suggest that soils from group 6 with large amounts of C in the subsoil might be losing C at a significant rate (Table 5). In fact, these were the conclusions reached by Kemanian and Stockle (2010) when simulating the C_s balance of the long-term experiment at Pendleton: no matter how much the inputs and mixing of the topsoil were manipulated, the subsoil seemed to lose carbon in those profiles. Here, and based on the simulations, a regression of initial subsoil C_s against the C rate of change indicates that the subsoil reaches steady-state regime at about 44 Mg C ha^{-1}, much less than the average of 75 Mg C ha^{-1} found throughout the farm. Only 10% of the farm area has subsoil C_s < 44 Mg C ha^{-1}.

The annual C_s balance compared with the annual C flux is relatively minor and therefore subject to errors. The humification rates estimated with the model are numerically lower than other reports but include rhizodeposition which was assumed to have a lower humification rate. The estimated turnover rates for C_s are low, less than 1% yr^{-1} for topsoil, and less than 0.3% yr^{-1} for the subsoil (Table 5). For the C_s in the subsoil to be stable, the carbon input rates from roots should be significantly higher than that simulated (unlikely), or the turnover rate of the soil much lower (feasible, but we found no evidence to sustain that assertion), or the humification rates much higher than those estimated (that would imply high microbial respiration efficiency or a rather limited microbial cycling), or significant mixing of soil layers that can transfer C_s form the topsoil to the subsoil. The latter is difficult to justify, and in addition, will cause C "loses" in the topsoil. It seems that lack of understanding C_s cycling in the subsoil is a major limitation to assess the overall C_s balance of soils in the Palouse and perhaps elsewhere. Cycling of C_s in the subsoil needs to be considered when discussing the impact of the conversion of these systems to no-till, or a sequence of no-till with period inversion tillage (Purakayastha et al., 2008).

Table 4. Simulated water balance as an average of 50-yr in the Cook Agronomy Farm in eastern Washington. The rotation was winter wheat – spring barley – spring wheat.The soil was tilled with one soil inversion operation with moldboard plow every 2 years.

Group	Runoff	Infiltration	Drainage	Evap. soil	Evap. Snow	Evap. residue	Transpiration
	---------- mm yr^{-1} ----------						
2	10	476	21	230	42	15	224
4	10	475	22	231	43	15	222

6	17	472	27	235	38	16	210

Table 5. Simulated soil organic carbon (C_s) balance as an average of 50-yr in the Cook Agronomy Farm in eastern Washington. The rotation was winter wheat – spring barley – spring wheat. C_i, h, and k as in Eq. [1]; C humified is the product hC_i on average for the 50 years. The C_s balance was obtained by regression and may differ slightly from calculations based on C_i, h, k, and C_s in Table 3. The C respired from residues is $(1 - h)C_i$, and is not presented in the table.

Group	Depth	C_i	C humified	h	C_s respired	k	C_s balance
	m	Mg ha^{-1} yr^{-1}		yr^{-1}	Mg ha^{-1} yr^{-1}	yr^{-1}	Mg ha^{-1} yr^{-1}
2	0 – 0.3	3.12	0.444	0.14	0.352	0.007	**0.099**
	0.3 – 1.5	0.22	0.026	0.12	0.052	0.001	-0.022
4	0 – 0.3	3.10	0.415	0.13	0.426	0.007	-0.003
	0.3 – 1.5	0.22	0.026	0.12	0.149	0.002	**-0.117**
6	0 – 0.3	3.00	0.400	0.13	0.449	0.007	-0.043
	0.3 – 1.5	0.22	0.028	0.13	0.310	0.003	**-0.275**

CONCLUDING REMARKS

The soil carbon distribution in the topsoil and subsoil at the CAF shows overall an expected pattern of erosion of convex and upland locations in the landscape, and accumulation of soil organic carbon in concave and lowland locations. Locally, however, describing a point as upland or lowland landscape position provides limited information to predict total C_s or its distribution with depth The topsoil C_s content is coupled with the local aboveground productivity, indicating that carbon inputs play a role at maintaining the current C_s across the landscape. No such relationship was found for subsoil C_s. Based on simulations of soil carbon accretion and cycling, much of the topsoil C_s can be at equilibrium with inputs, but the subsoil could be losing carbon a slow but steady rate for much of the farm. This is clearly an area that needs more research.

REFERENCES

Breiman, L. 2001. Random forests. Machine Learning 45:15–32.

Breiman, L., J. H. Friedman, R. A. Olshen, and C. J. Stone. 1984. Classification and regression trees. Wadsworth and Brooks/Cole, Monterey, California, USA.

Busacca, A.J., and J.A. Montgomery. 1992. Field-landscape variation in soil physical properties of the Northwest dryland crop production region. In Veseth, R. and B. Miller (ed.), Precision Farming for Profit and Conservation. 10th Inland Northwest Conservation Farming Conference Proceedings, Washington State University, Pullman.

Clay, D.E., C.G. Carlson, S.A. Clay, D.D. Malo. 2005. Soil organic carbon maintenance in corn (*Zea mays* L.) and soybean (*Glicine max* L.) as influenced by elevation zone. JSWC 60:342-348.

Gallant, J.C. and J.P. Wilson. 2000. Primary topographic attributes. p 51-85 In J.P. Wilson and J.C. Gallant (ed.) Terrain analysis: principles and applications. John Wiley & Sons Inc., New York, NY.

Huggins, D.R. and R.D. Alderfer. 1995. Yield variability within a long-term corn management study: implications for precision farming. p. 417-426. In P.C. Robert, R.H. Rust, and W.E. Larson (ed.) Site-Specific Management for

Agricultural Systems. Proc. of the 2nd Int. Conf., Minneapolis, MN. 27-30 March 1994. ASA, CSSA, and SSSA, Madison, WI.

Huggins, D.R., C.E. Clapp, R.R. Allmaras, J.A. Lamb, and M.F. Laysee. 1998a. Carbon dynamics in corn-soybean sequences as estimated from natural Carbon-13 abundance. SSSAJ 62:195-203.

Huggins, D.R., G.A. Buyanovsky, G.H. Wagner, J.R. Brown, R.G. Darmody, T.R. Peck, G.W. Lesoing, M.B. Vanotti, L.G. Bundy. 1998b. Soil organic C in the tallgrass pairie-derived region of the corn belt: effect of long-term crop management. Soil and Tillage Res. 47:219-234.

Kemanian, A.R., and C.O. Stöckle. 2010. C-Farm: A simple model to estimate the carbon balance of soil profiles. Europ. J. Agron. 32:22-29.

Liaw A. and M. Wiener, 2002. Classification and regression by randomForest. R News Vol 2/3:18-22.

Prasad A.M, L.R. Iverson, and A. Liaw, 2006. Newer classification and regression tree techniques: Bagging and Random Forests for ecological prediction. Ecosystems 9:181-199.

Purakayastha, T.J., D.R. Huggins, J.L. Smith. 2008. Carbon sequestration in native prairie, perennial grass, no-till, and cultivated Palouse silt loam. Soil Sci. Soc. Am. J, 72(2): 534-540.

Rasmussen, P.E., S. L. Albrecht and R.W. Smiley, 1998. Soil C and N changes under tillage and cropping systems in semi-arid Pacific Northwest agriculture. Soil and Tillage Research, 47:197-205.

Rehfeld, G.E., N.L. Crookston, M.V. Warwell, and J.S. Evans, 2006. Empirical analyses of plant-climate relationships for the western United States. Int. J. Plant Sci. 167:1123-1150.

Stockle, C.O., M. Donatelli, and R. Nelson, 2003. CropSyst, a cropping systems simulation model. Europ. J. Agronomy 18:289-307.